Microchemical Journal 103 (2012) 68–73

Contents lists available at SciVerse ScienceDirect

Microchemical Journal

journal homepage: www.elsevier.com/locate/microc

Antimony coordination to humic acid: Nuclear magnetic resonance and X-ray absorption fine structure spectroscopy study

Tserenpil Sh [a,*], Cong-Qiang Liu [a], Lihua Wang [b]

[a] State Key Laboratory of Environmental Geochemistry, Institute of Geochemistry, CAS, 550002 Guiyang, China
[b] Synchrotron Radiation Facility, Shanghai Institute of Applied Physics, CAS, 201204 Shanghai, China

ARTICLE INFO

Article history:
Received 12 December 2011
Received in revised form 13 January 2012
Accepted 13 January 2012
Available online 18 January 2012

Keywords:
Antimony-humic acid composite
^{1}H NMR spectroscopy
Solid state ^{13}C NMR spectroscopy
XAFS spectroscopy

ABSTRACT

This current study examined the fate of antimony (Sb) in the soil environment and its association with soil humic acid (HA). It is anticipated that a significant proportion of Sb is retained in soil organic layer; therefore, the oxidation state of Sb is controlled by the soil HA to some extent which influences Sb solubility and ecotoxicity. Parent HA material as well as prepared HA–Sb (III) composites was investigated by determining elemental composition and by performing nuclear magnetic resonance (NMR) and X-ray absorption fine structure (XAFS) spectroscopy study in order to study Sb coordination to natural macro organic ligand. The Sb (III) binding to soil derived HA mainly contributed to its open chains through carboxyl and hydroxyl moieties as revealed by the ^{1}H and solid state ^{13}C NMR spectroscopy. The protons in carboxylic and hydroxylic groups (those proton signals are characteristic of HAs with different origins) disappeared in the HA–Sb composite; and relative changes were observed in aliphatic proton distribution between the HA samples with and without Sb. The overall patterns of ^{13}C NMR spectra for the investigated samples were analogous to each other; moreover, it was estimated that the cyclic structure of the HA nucleus remained unchanged during Sb (III) association. Based on the absorption edge energy and coordination numbers, Sb oxidation state in a native soil was interpreted as pentavalent, meanwhile the HA–Sb composite contained both Sb (III) and Sb (V). It was shown that HA catalyzes Sb (III) oxidation to Sb (V) but the process was relatively slow. However, XAFS spectra sensitivity was limited when studying the HA–Sb composite that was prepared from the isolated soil HA fraction, so only data on the first shell Sb–O coordination were interpreted.

1. Introduction

In the soil system, humic substances are the most chemically active compounds with high cation and anion exchange capacities, and are long lasting, key components of soil. The complexing ability of procedurally defined HA fraction is equal to or greater than other fractions of humic substances and HA influences the speciation and mobility of metals.

On the other hand, the toxicity and distribution of the inorganic pollutants strongly depend upon their particle size and oxidation state. Typically fine particulates from smelter emission have a longer life time in aerosols [1] and pollution could be dispersed in an area stretching far away from the point source. Anthropogenic Sb deposits are most likely to be found in the terrestrial environment, as more is released to the land than to the water [2]. Unfortunately, Sb association with soil phases is not fully understood and it is often reported that Sb remains largely immobile and found in a residual fraction. Therefore, understanding the binding mechanism of Sb to soil derived HA may be important to the fate of Sb in the soils and for conducting risk assessments of contaminated soils.

The geochemistry of Sb in different environmental systems is not fully understood as the reduced form (i.e., Sb III) occasionally exists in an oxidized condition, and the oxidized form (i.e., Sb V) occasionally exists in a reduced condition. Further, it is often complicated to explain due to the strong hydrolysis of both tri- and pentavalent species in the typical environmental pH media. Concurrently with its unknown geochemical behaviors, a determination of organic and inorganic species of Sb in the different natural compartments as well as at geologically concentrated and anthropogenically accumulated sites needs to be carried out in order to understand Sb cycling, to predict its mobility and to develop detoxification procedure. As for arsenic, the organic form of Sb is less toxic than inorganic species and its toxicity decreases from Sb (III) to (V) [3]. Previous studies mostly dealt with Sb binding to inorganic ligands, but few studies exist on binding to organic ligands.

Due to the very complex multifunctional structure of HA, the mechanism of Sb bound to bulk HA (without fractionation of dissoluble and insoluble phases) and the molecular structure of Sb bearing complexes are not well documented. A structural study on Sb association to dissolved organic matter in an aquatic environment was

* Corresponding author.
E-mail address: tserenpil.sh@gmail.com (Sh. Tserenpil).

0026-265X/$ – see front matter © 2012 Elsevier B.V. All rights reserved.
doi:10.1016/j.microc.2012.01.006

conducted by Tella and Pokrovski [4], while Sb (III) binding mechanism to dissoluble fraction of HA was described by Buschmann and Sigg [5]. Previous studies showed that Sb (III) tends to interact with organic ligands more than Sb (V), and as a borderline metal, Sb (III) might possibly interact with both a soft ligand such as thiol (−SH) and a hard ligand like carboxyl (−COOH) groups.

XAFS spectroscopy is a powerful approach to investigating metal speciation, and its Fourier transform yields the radial distribution of atoms around a selected atom. However, Sb K-edge XAS has rarely been utilized for Sb compounds, and mostly used its aqueous solutions; for instance, in elucidating its complexation with chloride and sulfide [6-8]. Only a few studies conducted on heavily polluted bulk soil [9,10]. A recent survey conducted on Sb complexation with some sample organic ligands suggested that Sb forms complexes with both types of natural organic matter (e.g., HA and non HA), implying that a significant proportion of Sb is likely to be bound with HA via hydrocarboxylic moieties, in the form of bidentate complexes [4]. The chemical oxidation effect of HA is well known, and it catalyzes Sb (III) oxidation as well [5]. In contrast, the existence of reduced Sb form in an oxidized condition implies that the species could be stabilized by HA [11].

The coordination chemistry of Sb has both a theoretical and practical interest. The purpose of this study was to determine the moieties that contribute to Sb binding with HA molecules. This study also emphasized Sb (III) stabilization by HA. X-ray absorption near edge structure (XANES) spectroscopy's sensitivity to the atomic species enabled us to ascertain this behavior. These research objectives are expected to illuminate some uninvestigated behaviors of Sb geochemistry in soil systems, and Sb coordination with natural organic matter, since understanding and predicting environmental reactivity require detailed molecular information [12].

2. Materials and measurements

2.1. Sample description

In 2009, soil specimens from various depths were collected at a Sb smelting site in Guangxi Zhuang, China (for details, see [13]). From those, a soil profile of 30–40 cm (at site 1), which is less affected by the smelting activity, was taken for HA extraction. The HA fraction was isolated from demineralized soil using a sodium hydroxide (NaOH) extraction. For HA purification, the alkaline suspension was decanted, followed by centrifugation at a high speed of 10,000 rpm. HA precipitated at the pH of 2 from the alkaline extract and it was then washed before freeze drying. An HCl/HF treatment was not employed to avoid a destruction of HA molecular structure, and also because its ash content was not high. Further, HA–Sb composites were obtained by a direct reaction between Sb (III) (in the form of $C_4H_4KO_7Sb$) and isolated soil derived HA. Three trials were taken with different added Sb (III) amounts, which were 12, 71 and 143 $mg \cdot g^{-1}$ HA. Here, the bulk HA fraction was dissolved in alkaline solution and reacted with Sb (III) under 40 °C for 15 min. Newly formed composites were then precipitated by adding ethanol. A resultant composite with the maximum Sb binding of 253 $\mu mol \cdot g^{-1}$ (when the added Sb amount was 71 $mg \cdot g^{-1}$ HA) was taken for the XAFS measurements. Some investigated characteristics and compositions of parent HA and HA–Sb were used, as determined in the previous study [13]. In addition, two soil samples polluted by smelter emissions were taken for the XAFS study. However, only the Sb concentration of 3328 $mg \cdot kg^{-1}$ (at Site 2) was sufficient for the XAFS, while 760 $mg \cdot kg^{-1}$ (from Site 1) was not.

Antimony trioxide (Sb_2O_3) and antimony (III) potassium tartrate ($C_4H_4KO_7Sb$) were taken as the reference phases for the XAFS data acquisition and were purchased from Strem Chemicals (Newburyport, USA) and Tianjin \Chemicals (China), respectively. All the reagents were analytical reagent grade and purity was higher than ≥99.0%. In the NMR study, dimethyl sulfoxide-d_6 (DMSO-d_6) with isotopic purity >99.96 at.% D was supplied by Sigma Aldrich.

2.2. Data collection

2.2.1. ^1H NMR and solid state ^{13}C NMR spectroscopy

NMR spectroscopy is an effective method for the characterization of the chemical nature and relative abundance of functional groups of HA. It gives reliable results when atomic distributions are compared among materials coming from similar sources.

Original soil derived HA and the obtained HA–Sb composites were examined by both ^1H in DMSO-d_6 and solid state ^{13}C NMR spectroscopy. ^1H NMR spectra were acquired at 400 MHz with a Varian INOVA spectrometer fitted with a multinuclear probe. The Presat program was used for 1D acquisition of ^1H spectra with an acquisition time of 3.199 s and 1280 scans. Solid state ^{13}C NMR spectra were obtained using the cross polarization pulse program with two pulse phase modulated (TPPM15) decoupling on a Bruker AV 300 with ^{13}C resonating at 75 MHz. Dry and pulverized samples were placed in a 4 mm NMR rotor and sealed with a Kel-F cap. The spectra were recorded at a spinning speed of 12 kHz and samples were spun at the magic angle (54.7°) with a contact time of 3.0 ms and a 5 s recycle delay. Interpretation of ^1H and solid state ^{13}C NMR spectra was conducted based on the studies of soil HA [14,15]. The aromaticity of the HA molecule was calculated from ^{13}C NMR data by relating the content of aromatic carbons to the total content of aliphatic and aromatic carbon atoms.

2.2.2. XAFS spectroscopy

The X-ray absorption data at the Sb K-edge of the samples were recorded at the beamline BL 14W1 of Shanghai Synchrotron Radiation Facility (SSRF) in China. Both the X-ray absorption near edge spectroscopy (XANES) and extended X-ray absorption fine structure (EXAFS) were recorded. The station was operated with a Si (311) double crystal monochromator and the photon energy was calibrated with the first inflection point of Sb K-edge (30.5 keV) in Sb metal foil. During the measurement, the synchrotron was operated at energy of 3.5 GeV and a current between 150 and 200 mA. The reference phases (i.e., Sb_2O_3 and $C_4H_4KO_7Sb$) and the investigated samples (i.e., the HA–Sb composite and the surface soil sample) were oven dried and grounded then sieved (100 mesh) to ensure the small size of particles. Powder samples were spread evenly onto a 3M tape and used for the spectra collection. The reference samples were measured in transmission mode and the studied samples in fluorescence mode using a 4 element silicon drift detector at room temperature. Two scans were collected for each sample in order to get better signal to noise ratios. Here, it should be noted that the HA–Sb composite was stored in ambient condition for 10 months (from Sept, 2010) away from direct sunlight until the XAFS spectroscopy study (to June, 2011).

2.2.3. XAFS data treatment

XANES spectra were analyzed using the ATHENA program in IFEFFIT package [16]. The background was subtracted by the linear equation that was fitted to the region below the absorption edge and a polynomial function of degree 2 that was fitted to the EXAFS region. Then the spectra were normalized by the cubic spline method and the two scans were merged. After that, EXAFS spectra were analyzed using the conventional procedure with the aid of ATHENA and ARTEMIS programs. EXAFS oscillations, $\chi(k)$, were first extracted from the spectra and transformed from k-space (k^2, $k_{min} = 2.5$ Å^{-1}, $k_{max} = 10.0$ Å^{-1}) to R-space using a Hanning window to obtain the radial structure function (RSF). The EXAFS spectrum for the first shell was isolated by the inverse Fourier Transform (FT) of the RSF over the appropriate region and fitted using the single scattering EXAFS equation in both k- and R-space. The amplitude and phase

functions of Sb–O used for fitting were generated using the FEFF8.2 program from Sb_2O_3 and Sb_2O_5 and for the soil (Site 2) and HA–Sb. The residue used to evaluate the quality of the fits was the square root of the average square difference between the simulation and experimental data. And the S_0^2 was kept as a constant of 0.75 which was calculated with the EXAFS spectrum of Sb_2O_3.

3. Results and discussion

3.1. Characterization of HA and HA–Sb composite and ^1H and solid state ^{13}C NMR spectroscopy data

In order to be able to discuss Sb association to the HA macromolecule, the results on elemental compositions of the soil derived HA and HA–Sb were introduced here from the earlier study [13]. The bulk HA contained 8.8% ash, while the HA–Sb contained up to 35.6% clearly indicating its enrichment with inorganic components. The samples were composed of 48.4 and 43.6–47.2% C, 42.1 and 43.3–47.9% O, 5.9 and 5.8–6.3% H, 3.0 and 2.2–2.6% N and 0.7 and 0.5–0.6% S (in ash free basis), respectively. The carboxyl and hydroxyl groups in HA were determined by chemical analysis and the contents were respectively 438.85 $cmol \cdot kg^{-1}$ and 119.8 $cmol \cdot kg^{-1}$ (as phenolic –OH). Also, the results of ultimate analyses revealed the presence of other functional groups such as sulfur and nitrogen bearing units. Among the NMR spectra of the resultant HA–Sb composites, the spectrum for a composite (labeled S2-HA) with a Sb concentration of 30.87 $mg \cdot g^{-1}$ (or 253 $\mu mol \cdot g^{-1}$) HA was shown here as it contained the highest concentration of Sb and was taken for XAFS spectroscopy. ^1H NMR spectra of the soil derived HA and HA–Sb composite were compared and are shown in Fig. 1.

In the aliphatic proton region (between 0.8 and 3.6 ppm) of the ^1H NMR spectra (see Fig. 1), the resonance centered at around 0.834–0.837 ppm (which typically appears at 0.9 ppm) can be assigned to the protons of terminal methyl groups in alkyl chains. Protons in methyl groups of branched aliphatic chains and methylene groups of polymethylenic structure often occur at 1.3 and 2.1 ppm. These signals appeared at 1.219 and 2.073 in bulk HA (Fig. 1a), and at 1.222 ppm for the HA–Sb composite, with the second group disappearing for the HA–Sb (see Fig. 1b). Interestingly, an intense peak in the region of 1.038–1.041 ppm emerged in all of the HA–Sb composites, which was not observed in the HA sample. These differences of ^1H NMR spectra may originate from aliphatic protons which are directly and indirectly bound to Sb. The peaks at 1.4–1.8 ppm originate from protons on aliphatic carbons which are two or more carbons removed from aromatic rings or polar electronegative functional groups. Signals centered at 1.445 and 1.655 ppm were observed in this region as small peaks in bulk HA, and these were intensified and shifted upfield (respectively, 1.493 and 1.722 ppm) in the HA–Sb composite. The resonance at 1.8–3.0 ppm is believed to be protons attached to aliphatic carbons which are attached to electronegative functional groups (e.g. carboxyl groups or aromatic rings); however, the signals in this region affected by 2.490 ppm corresponds to DMSO-d_6. The short and broader signal at 3.440 ppm corresponds to protons on carbons attached to oxygen or nitrogen atoms in carbohydrates HOC, lignin methoxyl, protein amine or amino groups (HA contained 3% of N) and was observed in all HA–Sb samples but not in the HA. Finally, signals in the 6.0–10.0 ppm region can be assigned to multifunctional groups such as unhindered aromatic protons, phenols, carboxylic and amide N–H protons; however, a broad hump with the maximum at 8.308 ppm was assigned to protons in carboxylic acid and a peak at 7.219 ppm was assigned to phenolic moiety. The relative intensities of these signals were dramatically decreased (see Fig. 1b) for the HA–Sb composites from the elimination of exchangeable hydrogens in phenolic and carboxylic groups. This mechanism was formulated earlier on Sb binding to the HA molecule [4] and these authors showed that Sb (III) complexation was negligible with mono functional low molecular organic ligands or those having non adjacent carboxylic groups. In contrast, stable complexes were formed in the presence of polyfunctional carboxylic, hydroxy carboxylic acids and catechol over a wide range of pH.

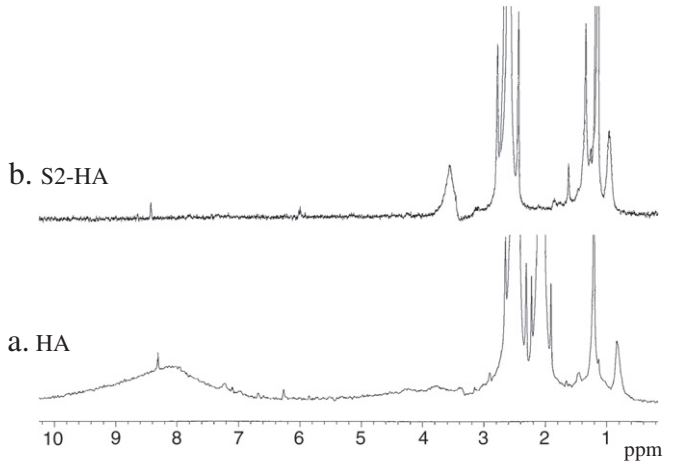

Fig. 1. ^1H NMR spectra of (a) soil derived HA and (b) HA–Sb composite (the peak at 2.489 ppm and its shoulders at 2.659 and 2.317 ppm correspond to DMSO).

Peak assignments and their relative percentage of peak areas of the ^{13}C NMR spectra are tabulated in Table 1. Resonance data disclosed that the both bulk HA and HA–Sb composite were dominated by aromatic (90–165 ppm) and carboxyl carbon (165–190 ppm) signals (Fig. 2). Aromaticity indicated that HA–Sb composite's condensed aromatic ring structure is similar to original HA and were 63.39 and 66.88, respectively (Table 1). It was also determined by an identical E_4/E_6 ratio (absorbance ratio at 465 nm and 665 nm) of 5.1 and 5.4 for HA and HA–Sb, respectively [13].

In general, similar patterns were depicted in the ^{13}C NMR spectra of the bulk HA and HA–Sb. Only slight changes were observed for the carbon atom distributions for individual functional groups. For instance, the integrated area of peaks at 165–90 ppm, that are assigned to H, C, N, O-substituted aromatic carbons, was lower in the HA–Sb composite than in the parent material by 6 units. This could have resulted from the calculations, for example when distributions of carbon atoms (for certain functional groups) truly increased while others were estimated to be as decreased within the total ^{13}C nuclear concentrations. The signals for carbonyl (small broad peaks) increased while the signals for carboxyl (maximum at 175 ppm) groups decreased insignificantly in the HA–Sb composite compared with the HA. This may be because certain moieties contributed to Sb association with HA by excluding its some units or elements, and from these form other groups by increasing their total content. And more significant decrease was observed in alkyl carbon which attached H or C atoms (ranging up to 50 ppm). This was consistent with significant resonance changes of alkyl hydrogen in the HA structure after binding Sb. A characteristic peak at 128 ppm was observed in the investigated samples and arose from protonated aromatic carbon at least two bonds away from O-substituted aromatic carbon [17]; while peaks were not characteristic at 115 ppm, 144 ppm and 153 ppm regions, which are assigned to protonated aromatic carbon in ortho or para to aromatic-O carbon, to O-substituted aromatic carbon of the dihydric (or methoxy) phenols and to monohydric phenolic carbon, respectively [17,18]. In Fig. 2, the peak at around 103 ppm (for both HA and HA–Sb composite) originated from anomeric carbon in polysaccharides and the well defined peaks at 73 ppm can be assigned to carbons in CH(OH) groups, ring carbons of polysaccharides and ether bonded aliphatic carbons. Hence, it may be that the identified soil HA is relatively rich in carbohydrates.

Table 1
Relative intensity distribution in the solid-state ^{13}C NMR spectra of the soil-derived HA and HA–Sb composite.

Sample	Relative intensity of functional groups, %							Aromaticity
	$C_{C=O}$ 220–190 ppm	C_{COO} 190–165 ppm	$C_{Ar-O,\ N}$ 165–135 ppm	$C_{Ar-H,\ C}$ 135–90 ppm	$C_{Alk-O,\ N}$ 90–60 ppm	$C_{CH\ O}$ 60–50 ppm	$C_{Alk-H,\ C}$ 50–0 ppm	
HA	2.17	10.34	14.66	28.48	9.06	2.96	9.34	66.88
HA–Sb	3.07	9.23	12.75	24.31	11.96	2.70	6.47	63.39

Interpretation from both ^{1}H NMR and ^{13}C NMR spectroscopy showed that phenolic hydroxyl, carbonyl and carboxyl in the HA macromolecule possibly contributed to Sb binding to soil HA.

3.2. XAFS spectroscopy data on the soil derived HA and HA–Sb composite

Sb (V) is a thermodynamically stable oxidation state and it prevails in the variable soil environments [19]. However, Sb (III) also has been found in both oxidized and reduced conditions. Therefore, XAS spectra were acquired on the HA–Sb organometal composite and the native soil with highly elevated Sb concentration in order to study Sb binding to its neighboring atoms and to ascertain if the reduced Sb form could be stabilized by organic ligands like HA.

Figs. 3–5 and Table 2 give the XANES and EXAFS spectra and fit results measured in the reference phases and the studied materials. The XANES spectra of the soil have a higher absorption edge energy (30,497 eV) compared to the edge energy of 30,493 eV and 30,494 eV for the reference compounds containing Sb (III), while the absorption edge was less pronounced at 30,491 eV for Sb metal foil. For the HA–Sb composite, the edge energy was measured as 30,494 eV.

Scheinost et al. [19] have confirmed that the tri- and pentavalent oxidation states of Sb can be distinguished by the edge energy differences of 4 eV and based on their coordination numbers. Trivalent Sb can be discriminated from the higher oxidation states by their small O-peaks in the EXAFS Fourier transforms and fitted O-coordination numbers, which were around three and six for the tri- and pentavalent Sb, respectively. In this present work, the edge energy for the trivalent Sb was equal to that measured by Scheinost and their data was used for interpretation of the current results. The characteristics of the smelter polluted surface soil were similar to that of the pentavalent oxide of Sb, indicating that its oxidation state is virtually as Sb (V). This tendency was consistent with the data by Takaoaka [20] that showed that Sb (V) was the predominant species in the smelter polluted soil. But the absorption edge energy of the HA–Sb composite was intermediate compared to those for tri-and pentavalent oxides.

Fig. 4 shows the RSF with phase uncorrected for the reference materials and investigated samples. Based on the comparison, the nearest neighboring atoms were determined to be oxygen atoms and the major peak could be attributed to Sb–O bonds. The best fitting results in *k*-, *R*- and *q*-space of the surface soil at Site 2 and the HA–Sb composite are shown in Fig. 5. The fitting results both measured experimentally and as calculated values are illustrated. Structural parameters were calculated by the least squares fit of the inverse Fourier transformed EXAFS oscillations with k^2 weight, and shown in Table 2. For the surface soil samples, the first Sb shell yielded 6 oxygen atoms at a radial distance of 1.96 and around 4 oxygen atoms were calculated for the HA–Sb at 1.99 , again indicating that the composite contains a mixture of Sb (III) and Sb (V), which means that the initially taken Sb (III) partly converted to its higher oxidation state (Table 2). The process of Sb (III) oxidation to Sb(V) was fast via other soil constituents like amorphous manganese (Mn) and iron (Fe) oxyhydroxides; these isolated phases showed rapid and complete oxidation within 3 to 7 days [21]. All the findings confirm that the Sb (III) oxidation state may be maintained after its coordination to HA; however, HA also will catalyze Sb oxidation but it is relatively slow since the HA–Sb sample still contains some Sb (III) after 10 months of storage. This was also shown by Buschmann and Sigg [5] in an aqueous solution. In the true soil environment, it is probable that Sb interacts quickly with Fe and Mn oxyhydroxide phases and it oxidizes; hence Sb (V) interaction with HA also needs to be considered.

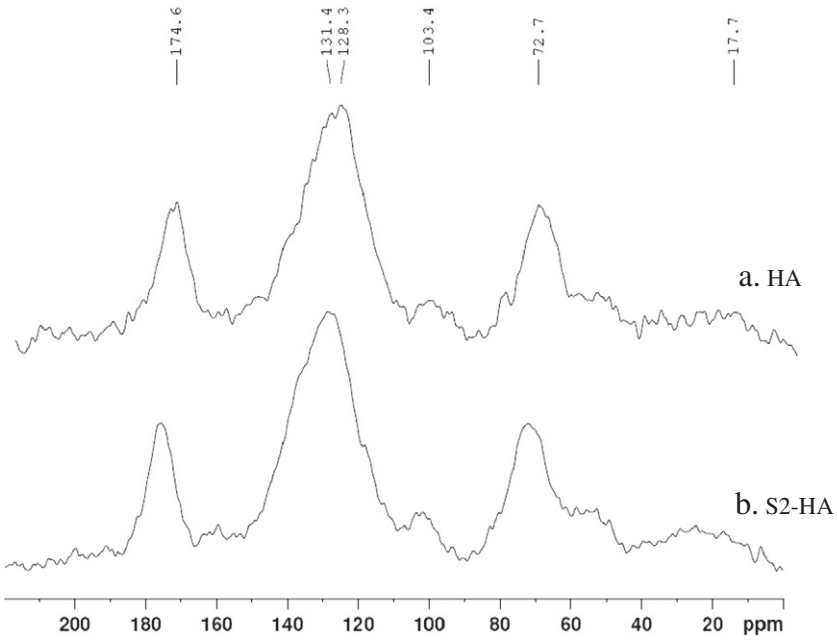

Fig. 2. Solid state ^{13}C NMR spectra of soil derived HA and HA–Sb composite (a. Soil derived HA; b. HA–Sb composite spectra).

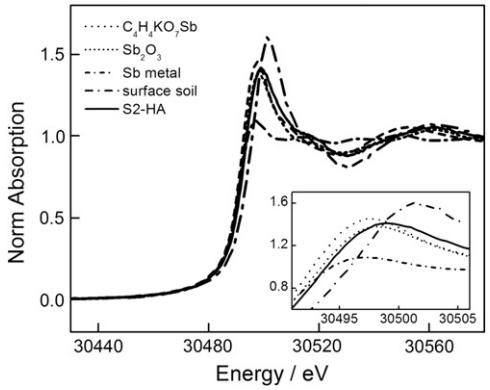

Fig. 3. Normalized Sb K-edge XANES spectra of the reference materials (Sb_2O_3, $C_4H_4KO_7Sb$ and Sb metal foil) and investigated samples (HA–Sb composite and the surface soil).

Scheinost et al. [19] expected to see the backscattering signals of C atoms (carboxylate groups in HA) at a distance of 3–3.5 in the sorption complex of HA with Sb but it did not occur. In the current study, the composite based on the isolated HA fraction was expected to show the signals in the above region but the sensitivity of the XAFS was insufficient to disclose this coordination, since this coordination was suggested by the NMR study. This was clearly due to the weak backscattering of C which masks existing complexation. Hence, not only the availability of existing coordination but also its intensity is important for the XAFS study.

4. Conclusions

HA–Sb (III) composites were prepared based on the bulk soil derived HA. The parent HA and HA–Sb composites were studied by elemental analysis and NMR spectroscopy. Further, Sb concentrations of the prepared HA–Sb composite and the polluted surface soil were 253 $\mu mol \cdot g^{-1}$ and 3328 $mg \cdot kg^{-1}$, and were sufficient to investigate by XAFS. The ^1H NMR resonance data on bulk HA and HA–Sb composite showed that hydrogen in carboxyl and phenolic OH groups decreased dramatically in the HA molecule after association with Sb atoms, and it has been speculated that aliphatic protons may also contribute to Sb binding directly and indirectly. In the ^{13}C NMR study, general distributions of aliphatic and aromatic carbon nuclei remained similarly independent if the HA sample does or does not contain Sb atoms. However, integrated areas of the peaks for different functional groups showed changes both increases and decreases, which may be caused by Sb association to HA. Sb (III) binding to soil derived HA mainly contributed to open chains through carboxyl and hydroxyl moieties as revealed by the ^1H and solid state ^{13}C NMR spectroscopy. The Sb oxidation state in the soil sample was

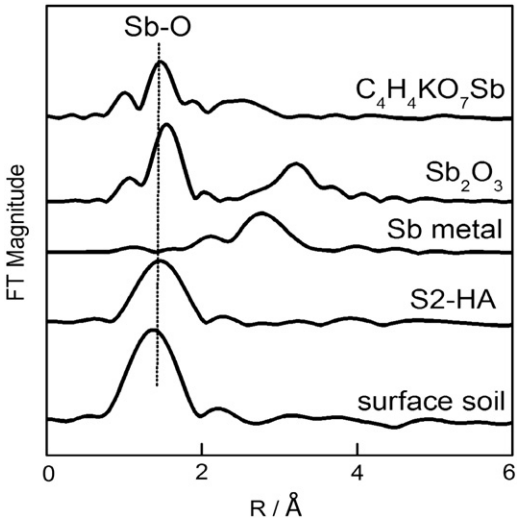

Fig. 4. Fourier-transform EXAFS spectra (no phase shift corrected) in references (Sb_2O_3, $C_4H_4KO_7Sb$ and Sb metal foil) and investigated samples (HA–Sb composite and the surface soil).

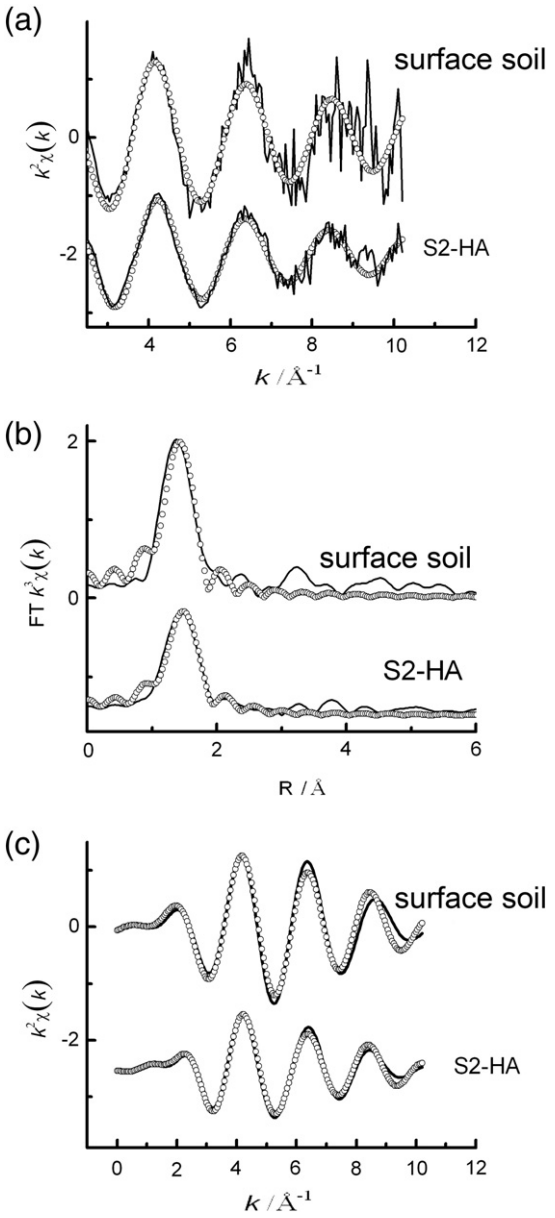

Fig. 5. The best fitting results in (a) *k*-, (b) *R*- and (c) *q*-space for the soil and HA–Sb composite (solid lines are for the experimental values and open circles are for the calculated values).

Table 2
Structural parameter for the soil sample and HA–Sb composite.

Sample	E_0 (eV)	Coordination shell			
		CN[a]	R( )[b]	σ^2(Å^2)[c]	R-factor[d]
Native soil	30,497	6.0 ± 1.5	1.96 ± 0.03	0.001 ± 0.004	0.02
HA–Sb composite	30,493	4.2 ± 0.4	1.99 ± 0.01	0.002 ± 0.001	0.008

[a] Coordination number.
[b] Inter-atomic distance.
[c] Debye–Waller factor.
[d] Scattering amplitude.

determined to be Sb (V) by the XANES and EXAFS data; while data for the HA–Sb composite showed that it contains both its reduced and oxidized species, which means that the initially taken Sb (III) was partly oxidized into Sb (V). The results suggest that HA catalyzes Sb (III) oxidation even in the solid phase, but the process is slow.

Acknowledgment

The authors would like to thank beamline BL14W1 (Shanghai Synchrotron Radiation Facility) for providing the beam time and to Prof. Zhang Jian Xin for acquisition of the NMR spectra. Finally, the author, TS strongly thanks Professors E. Jeppesen and S. Rothenberg for their constant support.

References

[1] M. Fierro, Particulate matter, www.airinfonow.com/pdf/Particulate_Matter.pdf2000.
[2] M. Filella, N. Belzile, Y.W. Chen, Antimony in the environment: a review focused on natural waters. I. Occurrence, Earth Sci. Rev. 57 (2002) 125–176.
[3] M. Krachler, W. Shotyk, H. Emons, Digestion procedures for the determination of antimony and arsenic in small amounts of peat samples by hydride generation atomic absorption spectrometry, Anal. Chim. Acta 432 (2001) 307–314.
[4] M. Tella, G.S. Pokrovski, Antimony (III) complexing with O-bearing organic ligands in aqueous solution: an X-ray absorption fine structure spectroscopy and solubility study, Geochim. Cosmochim. Acta 73 (2009) 268–290.
[5] J. Buschmann, L. Sigg, Antimony(III) binding to humic substances: influence of pH and type of humic acid, Environ. Sci. Technol. 38 (2004) 4535–4541.
[6] E.H. Oelkers, D.M. Sherman, K.V. Ragnarsdottir, C. Collins, An EXAFS spectroscopic study of aqueous antimony (III)-chloride complexation at temperatures from 25 to 250 °C, Chem. Geol. 151 (1998) 21–27.
[7] J.F.W. Mosselmans, G.R. Helzb, R.A.D. Pattrickc, J.M. Charnock, D.J. Vaugha, A study of speciation of Sb in bisulfide solutions by X-ray absorption spectroscopy, Appl. Geochem. 15 (2000) 879–889.
[8] D.M. Sherman, K.V. Ragnarsdottir, E.H. Oelkers, Antimony transport in hydrothermal solutions: an EXAFS study of antimony (V) complexation in alkaline sulfide and sulfide–chloride brines at temperatures from 25 °C to 300 °C at *P*sat, Chem. Geol. 167 (2000) 161–167.
[9] M. Takaoka, S. Fukutani, T. Yamamoto, M. Horiuchi, N. Satta, N. Takeda, K. Oshita, M. Yoneda, S. Morisawa, T. Tanaka, Determination of chemical form of antimony in contaminated soil around a smelter using X-ray Absorption fine structure, Anal. Sci. 21 (2005) 769–773.
[10] A.C. Sheinost, A. Rossberg, D. Vantelon, F. Xifra, R. Kretzschmar, A.K. Leuz, H. Funke, C.A. Johnson, Quantitative antimony speciation in shooting-range soils by EXAFS spectroscopy, Geochim. Cosmochim. Acta 70 (2006) 3299–3312.
[11] H.W. Sun, X.Q. Shan, Z.M. Ni, Selective separation and differential determination of antimony (III) and antimony (V) by solvent extraction with Nbenzoyl-Nphenylhydroxylamine and graphite furnace atomic adsorption spectrometry using a matrix modification technique, Talanta 29 (1982) 589–593.
[12] A.J. Simpson, D.J. McNally, M.J. Simpson, NMR spectroscopy in environmental research: from molecular interactions to global processes, Prog. Nucl. Magn. Reson. Spectrosc. 58 (2011) 97–175.
[13] Sh. Tserenpil, C.-Q. Liu, Study of Antimony (III) binding to soil humic acid from an antimony smelting site, Microchem. J. 98 (2011) 15–20.
[14] E. Montoneri, P. Savarino, F. Adani, P.L. Genevini, G. Ricca, F. Zanetti, S. Paoletti, Polyalkylphenyl-sulphonic acid with acid groups of variable strength from compost, Waste Manage. 23 (2003) 523–535.
[15] O.A. Trubetskoj, P.G. Hatcher, O.E. Trubetskaya, ^{1}H NMR and ^{13}C NMR spectroscopy of chernozem soil humic acid fractionated by combined size-exclusion chromatography and electrophoresis, Chem. Ecol. 26 (2010) 315–325.
[16] B. Ravel, M. Newville, Athena, Artemis, Hephaestus: data analysis for X-ray absorption spectroscopy using IFEFFIT, J. Synchrotron Radiat. 12 (2005) 537–541.
[17] P.G. Hatcher, Chemical structural models for coalified wood (vitrinite) in low rank coal, Org. Geochem. 16 (1990) 959–968.
[18] R.H. Newman, M.N. Sim, J.H. Johnstion, J.D. Collen, Comparison of aromaticity and phenolic content as parameters for characterization of coal by 13C n.m.r. spectroscopy, Fuel 67 (1988) 420–425.
[19] A.C. Scheinost, A. Rossberg, D. Vantelon, I. Xifra, R. Kretzschmar, A.K. Leuz, H. Funke, C.A. Johnson, Quantitative antimony speciation in shooting-range soils by EXAFS spectroscopy, Geochim. Cosmochim. Acta 70 (2006) 3299–3312.
[20] M. Takaoka, S. Fukutani, T. Yamamoto, M. Horiuchi, N. Satta, N. Takeda, K. Oshita, M. Yoneda, S. Morisawa, T. Tanaka, Determination of chemical form of antimony in contaminated soil around a smelter using X-ray absorption fine structure, Anal. Sci. 21 (2005) 769–771.
[21] N. Belzile, Y.W. Chen, Z. Wang, Oxidation of antimony (III) by amorphous iron and manganese oxyhydroxides, Chem. Geol. 174 (2001) 379–387.